Cell

Programmed Cell Senescence during Mammalian Embryonic Development

Daniel Muñoz-Espín,[1] Marta Cañamero,[2] Antonio Maraver,[1] Gonzalo Gómez-López,[3] Julio Contreras,[4,5,6] Silvia Murillo-Cuesta,[5,6] Alfonso Rodríguez-Baeza,[7] Isabel Varela-Nieto,[5,6] Jesús Ruberte,[8] Manuel Collado,[1,9] and Manuel Serrano[1,*]

[1]Tumor Suppression Group
[2]Histopathology Unit
[3]Bioinformatics Unit
Spanish National Cancer Research Center (CNIO), Madrid E28029, Spain
[4]Department of Anatomy, School of Veterinary Medicine, Universidad Complutense de Madrid, Madrid E28040, Spain
[5]Instituto de Investigaciones Biomédicas Alberto Sols, CSIC-UAM, Madrid E28029, Spain
[6]Centre for Biomedical Network Research on Rare Diseases (CIBERER), Valencia E46010, Spain
[7]Departament de Ciències Morfològiques, Facultat de Medicina
[8]Center for Animal Biotechnology and Gene Therapy (CBATEG), Department of Anatomy and Animal Health, School of Veterinary Medicine Universitat Autònoma de Barcelona, Bellaterra E08193, Spain
[9]Present address: Instituto de Investigación Sanitaria de Santiago de Compostela (IDIS), Complexo Hospitalario Universitario de Santiago de Compostela (CHUS), SERGAS, Santiago de Compostela E15706, Spain
*Correspondence: mserrano@cnio.es
http://dx.doi.org/10.1016/j.cell.2013.10.019

SUMMARY

Cellular senescence disables proliferation in damaged cells, and it is relevant for cancer and aging. Here, we show that senescence occurs during mammalian embryonic development at multiple locations, including the mesonephros and the endolymphatic sac of the inner ear, which we have analyzed in detail. Mechanistically, senescence in both structures is strictly dependent on p21, but independent of DNA damage, p53, or other cell-cycle inhibitors, and it is regulated by the TGF-β/SMAD and PI3K/FOXO pathways. Developmentally programmed senescence is followed by macrophage infiltration, clearance of senescent cells, and tissue remodeling. Loss of senescence due to the absence of p21 is partially compensated by apoptosis but still results in detectable developmental abnormalities. Importantly, the mesonephros and endolymphatic sac of human embryos also show evidence of senescence. We conclude that the role of developmentally programmed senescence is to promote tissue remodeling and propose that this is the evolutionary origin of damage-induced senescence.

INTRODUCTION

Cellular senescence is defined as a stable cell-cycle arrest elicited in response to multiple types of damage, such as intense oncogenic signaling, DNA damage, and telomere loss (Campisi and d'Adda di Fagagna, 2007; Collado et al., 2007). Senescent cells are found in association with pathological situations, most notably within tumors and in some aged tissues (Campisi and d'Adda di Fagagna, 2007; Collado et al., 2007). The tumor suppressors p16INK4a (abbreviated as p16), p19ARF, p53, and RB are critical for the establishment of senescence in most experimental settings (Campisi and d'Adda di Fagagna, 2007; Collado et al., 2007), although other senescence mediators have been identified (Gorgoulis and Halazonetis, 2010). For instance, cyclin-dependent kinase inhibitors p21 and p27 also contribute to senescent phenotypes (Collado and Serrano, 2010). In addition, senescent cells secrete a number of extracellular factors, including transforming growth factor β (TGF-β), IGF1-binding proteins, and inflammatory cytokines, that can reinforce and propagate senescence in an autocrine and paracrine manner (Acosta et al., 2013; Kuilman and Peeper, 2009). The senescence-associated secretory phenotype (SASP) can also evoke a local inflammatory response with complex effects, including the elimination of senescent cells by phagocytosis, thus leading to tissue remodeling and damage resolution (Freund et al., 2010; Hoenicke and Zender, 2012; Krizhanovsky et al., 2008).

Together with senescence, apoptosis is the other main cellular response to damage, and both processes can share common triggers, such as DNA damage or oncogenic stress, and common mediators, most notably p53 (Campisi and d'Adda di Fagagna, 2007; Collado et al., 2007; Vousden and Prives, 2009). Apoptosis in response to errors, insults, or pathological situations has been referred to as nonprogrammed cell death to reflect its accidental nature (Kourtis and Tavernarakis, 2007). Interestingly, apoptosis also plays an important role during animal development, where it occurs in a well-defined manner in response to developmental cues, and it is classically referred to as developmentally programmed cell death (Conradt, 2009; Fuchs and Steller, 2011; Kourtis and Tavernarakis, 2007).

We hypothesized that cellular senescence, like apoptosis, could also participate in embryonic development, i.e., in a

developmentally programmed manner. We report here the existence of widespread developmental senescence during mammalian development, and we focus on two embryonic structures, the mesonephros and the endolymphatic sac of the inner ear.

We took note of a previous report showing senescence-associated β-galactosidase (SAβG) activity in the regressing mesonephros of birds (Nacher et al., 2006), although this observation was not further characterized. SAβG is the most widely used assay to detect senescence both in vitro and in vivo (Collado and Serrano, 2006; Dimri et al., 1995), and it is based on the increased lysosomal content of senescent cells (Kurz et al., 2000). In mammals, the mesonephros is an elongated structure, adjacent to the gonads, and longitudinally crossed by the mesonephric or Wolffian ducts, from which numerous lateral tubules emerge (Sainio, 2003; Vazquez et al., 1998). The mesonephros functions as a transitory embryonic kidney before the maturation of the definitive kidney, or metanephros, and then it essentially disappears (Davidson, 2008).

We have also focused on the endolymphatic sac of the inner ear because we found that its SAβG activity is particularly prominent. The function of the endolymphatic sac is to collect and filtrate the endolymph of the cochlear and vestibular canals, which are involved in hearing and balance, respectively (Hultcrantz et al., 1987; Lo et al., 1997).

Here, we present a detailed analysis of developmentally programmed senescence at the mesonephros and at the endolymphatic sac, including the genetic identification of mediators and regulatory pathways, the manipulation of the senescence program with chemical agents, the analysis of clearance mechanisms and compensatory processes, and finally, the morphological consequences of abrogating programmed senescence.

RESULTS

Developmentally Programmed Senescence in Whole-Mount Embryos

We began by performing exploratory SAβG stainings in whole-mount mouse embryos at different developmental stages. Two intense SAβG signals were reproducibly observed near the ear canals from embryonic day 12.5 (E12.5) to E14.5 (Figure 1A, first picture from the left), which upon further analysis turned out to correspond to the endolymphatic sacs (abbreviated ES) (see below). A symmetric pattern of SAβG staining was also observed in the posterior cranium that corresponds to the closing neural tube (Figure 1A, first picture). SAβG signal was also found in the apical ectodermal ridge (AER) of the limbs at E11.5 (Figure 1A, second picture) and was at later times concentrated at the bottom of the regressing interdigital webs (Figure 1A, third picture). Moreover, SAβG staining was also obvious around the vibrissae (below the eye) (Figure 1A, fourth picture). Other sites positive for SAβG are listed separately (Table S1 available online). Similar findings are reported in the accompanying paper (Storer et al., 2013). Based on a previous report of SAβG activity in the mesonephros of the quail (Nacher et al., 2006), we dissected the gonad-mesonephros complex of mouse embryos and performed whole-mount staining, revealing a clear positive SAβG signal in the mesonephric tubules (Figure 1A, fifth picture). Therefore, cellular senescence, defined at this point on the basis of SAβG activity, is a frequent finding in whole-mount embryos.

Developmentally Programmed Senescence in the Mesonephric Tubules and Endolymphatic Sac

We decided to focus on the mesonephric tubules (Figure S1A) due to the evolutionary conservation of senescence in this organ from birds to mammals and on the endolymphatic sac (Figure S1B) because of its intense SAβG staining in whole-mount embryos. The involution of the mesonephros begins at E14.5, and within 24 hr, almost all the mesonephric tubules disappear in a caudal-to-apical direction (Davidson, 2008; Vazquez et al., 1998). Fresh whole-mount embryos at different developmental stages were subjected to SAβG staining and then were processed for paraffin inclusion, sectioned, and, when indicated, stained by immunohistochemistry. At day E11.5, the mesonephric tubules had no SAβG activity and were highly positive for the proliferation marker Ki67 (Figure 1B). However, from E12.5 to E14.5, SAβG activity was clearly detectable, and Ki67 staining was progressively reduced. Finally, at E15.5, most of the mesonephric tubules had disappeared and hardly, if any, SAβG staining was observed. Therefore, there is a strong association between SAβG activity and absence of proliferation, which together constitute a hallmark of senescence.

A similar pattern and kinetics were observed in the endolymphatic sac (Figure 1C). However, it is important to note that, in contrast to the mesonephros, in the case of the endolymphatic sac there is no regression. Previous investigators have reported that a minor fraction of cells within the endolymphatic sac undergo a rapid expansion beginning at E14.5 (Kim and Wangemann, 2011), and, as we will show further below, this is the most plausible explanation for Ki67 positivity at E15.5 in this organ.

The intensity of the SAβG signal in the E14.5 endolymphatic sac was noticeably higher than in the mesonephros, and we wondered whether this was due, at least in part, to the different accessibility of the β-galactosidase substrate (X-Gal) to the two structures when performing whole-mount staining. To address this, unstained frozen embryos embedded in OCT were serially sectioned, and the relevant sections containing the mesonephros and the endolymphatic sac were stained in parallel for SAβG (Figure 1D). Interestingly, under equal staining conditions, the intensity of the SAβG signal was comparable in both structures. This also indicates that the reduced accessibility of X-Gal to internal organs, such as the mesonephros, significantly decreases the intensity of the SAβG signal in whole-mount staining of embryos.

To further document senescence in the mesonephric tubules and endolymphatic sac, we used markers of senescence-associated heterochromatin (Narita et al., 2003) and observed that epithelial cells from both structures at E14.5 were positive for HP1γ (Figure 1E) and H3K9me3 (Figure S1C), whereas surrounding stromal cells were negative. In contrast, at E11.5, the epithelia of the mesonephric tubules and endolymphatic sac were negative or weakly positive for H3K9me3 (Figure S1C), thus following the same pattern as the SAβG staining. We also wondered whether senescent cells were arrested at G1 (or alternatively at G2), and for this, we stained with the centrosomal marker

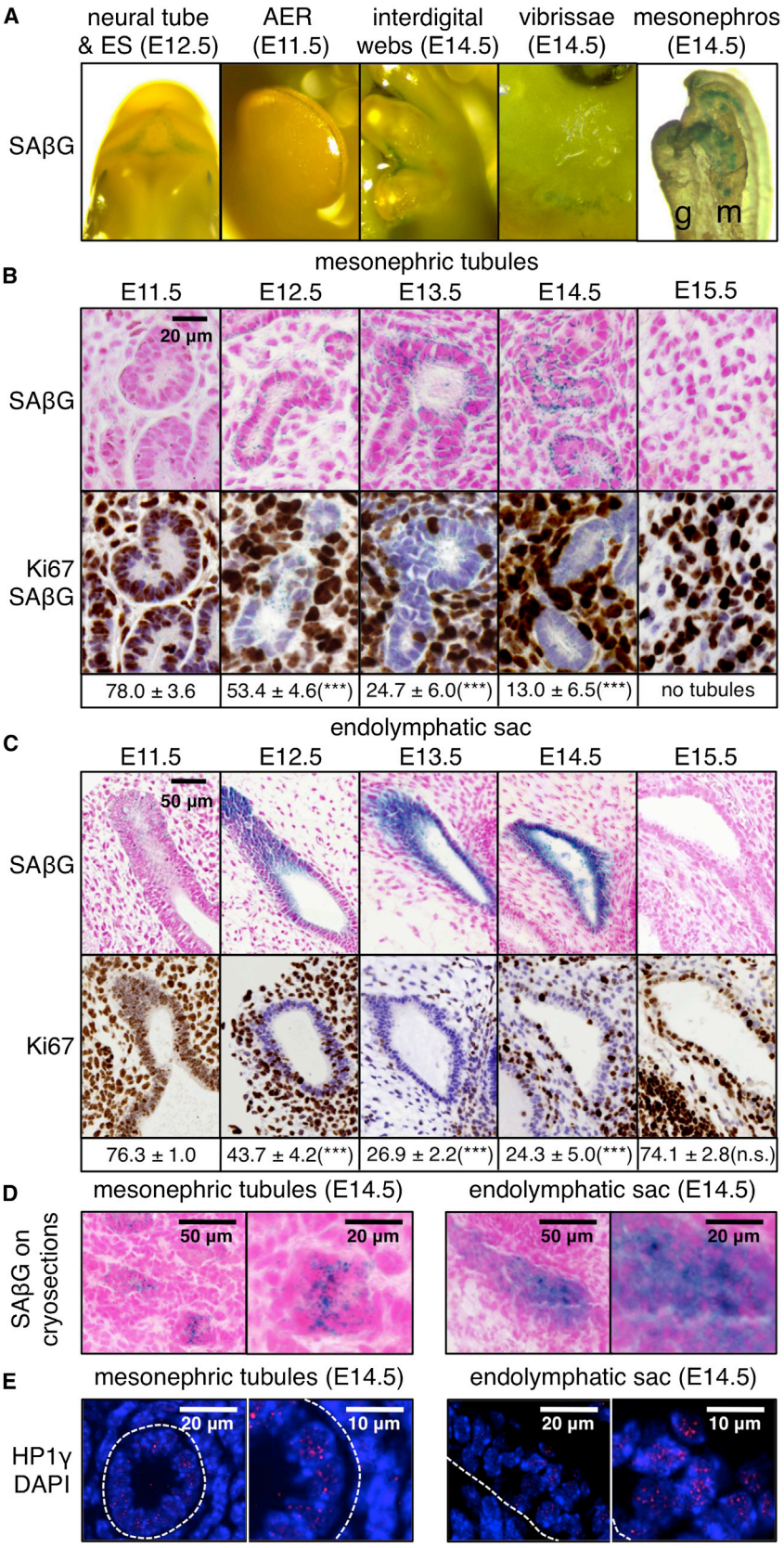

Figure 1. Programmed Senescence Occurs during Mouse Embryonic Development

(A) Examples of senescent structures after embryo whole-mount SAβG staining at the indicated stages. ES, endolymphatic sac; AER, apical ectodermal ridge.

(B) Whole-mount SAβG staining and Ki67 immunohistochemistry of mesonephric tubules at the indicated stages. The percentages of Ki67-positive cells in the mesonephric tubules are shown (E11.5, n = 4; E12.5, n = 3; E13.5, n = 3; E14.5, n = 7).

(C) Whole-mount SAβG staining and Ki67 immunohistochemistry of the endolymphatic sac at the indicated stages. The percentages of Ki67-positive cells at the endolymphatic sac are shown (E11.5, n = 3; E12.5, n = 5; E13.5, n = 5; E14.5, n = 10; E15.5, n = 4).

(D) Cryosections containing mesonephric tubules (left) and endolymphatic sac (right) stained with SAβG.

(E) HP1γ (red) immunofluorescence of a mesonephric tubule (left) and endolymphatic sac (right). The basal lamina of the two epithelia is indicated with a dotted white line. Nuclei were stained with DAPI (blue).

All samples correspond to WT embryos. SAβG and HP1γ stainings were performed in at least five embryos, obtaining the same result in all cases. In (B) and (C), values are expressed as mean ± SD, and statistical significance is relative to E11.5 embryos assessed by the two-tailed Student's t test: ***$p < 0.001$; n.s. (not significant).

See also Figure S1 and Table S1.

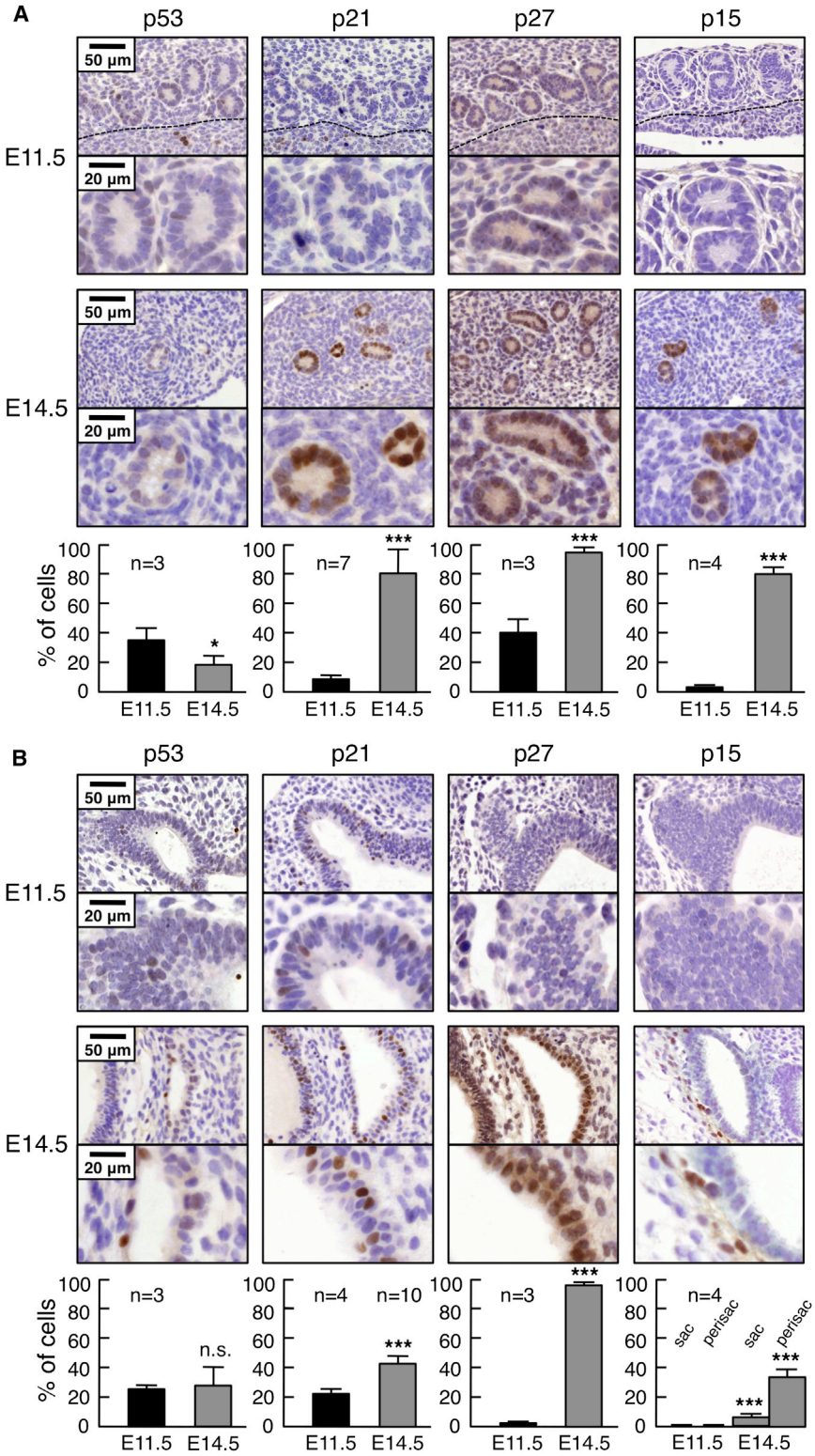

Figure 2. Expression of Cell-Cycle Inhibitors in the Mesonephric Tubules and Endolymphatic Sac

(A) Mesonephric tubules stained for p53, p21, p27, or p15. The graphs show the percentages of positively stained cells in the epithelia of the mesonephric tubules at E11.5 and E14.5. Dotted black lines, at E11.5, separate the mesonephros (upper part) from the gonad (lower part).

(B) Endolymphatic sacs stained as in (A). The graphs show the percentages of positively stained cells in the endolymphatic sac epithelia at E11.5 and E14.5. In the case of p15 staining, the graph shows the percentage of positively stained cells at both epithelial (sac) and perisacular (perisac) regions at E11.5 and E14.5. The picture exhibiting p15 staining at E14.5 corresponds to an embryo subjected to whole-mount SAβG staining to differentiate the epithelium from the perisacular region.

All samples correspond to WT embryos. Values are expressed as mean ± SD, and statistical significance was assessed by the two-tailed Student's t test: *$p < 0.05$; ***$p < 0.001$; n.s. (not significant); the total number of embryos analyzed is indicated in each graph (n).

See also Figure S2.

pericentrin. In both structures, we observed a single centrosome signal per cell, which is indicative of G1-phase arrest (Figure S1D). Finally, the mesonephric tubules and endolymphatic sac had negligible γH2AX levels that were even lower than those in the surrounding stroma (Figure S1E), thus indicating that DNA damage is not associated with senescence in these structures.

In summary, we document the occurrence of developmentally programmed senescence in the mesonephric tubules and in the endolymphatic sac, characterized by SAβG activity, senescence-associated heterochromatin markers, and absence of proliferation due to G1-phase arrest.

Expression of Senescence Mediators in the Mesonephric Tubules and Endolymphatic Sac

We also examined the expression of the most relevant mediators of senescence. Sections of E11.5 (low SAβG) and E14.5 (high SAβG) embryos were stained to detect p53, p21, p27, p15, p19ARF, and p16 (Figures 2A, 2B, and S2A). Positive, albeit weak, staining of p53 was detected in the epithelia of mesonephric tubules and endolymphatic sac, but its levels did not increase from E11.5 to E14.5. In contrast, staining for p21, p27, or p15 was significantly increased from E11.5 to E14.5 (Figures 2A and 2B). In the case of p27, expression at E14.5 was observed in the epithelia and in the surrounding stroma; and, in the case

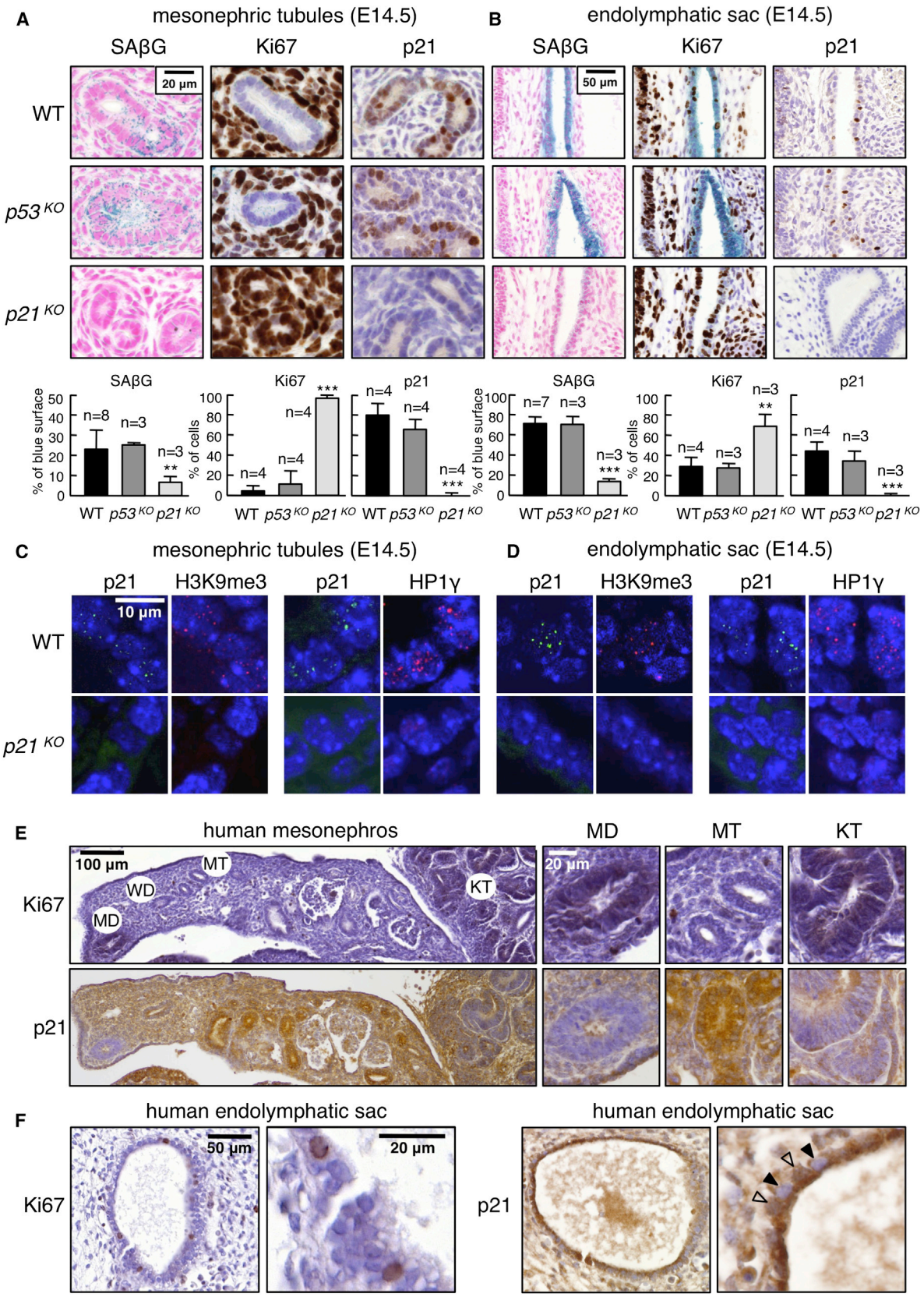

(legend on next page)

of p15, expression was more prominent in the perisacular stroma of the endolymphatic sac rather than in the epithelium. No evidence of expression was obtained for p19ARF or p16 in the mesonephros or endolymphatic sac (Figure S2A).

Developmentally Programmed Senescence Requires p21 Independently of p53

The functional relevance of the senescence mediators examined above was tested genetically. Despite the almost universal relevance of p53 in senescence (Campisi and d'Adda di Fagagna, 2007; Collado et al., 2007), the mesonephric tubules and endolymphatic sac of *p53* null embryos presented similar levels of SAβG activity and Ki67-negative cells as did wild-type (WT) embryos (Figures 3A and 3B). In contrast, these epithelia were almost completely devoid of SAβG activity, and most cells were positive for Ki67 in *p21* null embryos (Figures 3A, 3B, and S2B). Also, the levels of SAβG activity at the endolymphatic sac of *p21*-heterozygous embryos were intermediate between those in WT and *p21* null embryos (Figure S2C). These observations indicate that senescence is dependent on p21, but independent of p53. Accordingly, p21 levels were similar in both epithelial structures regardless of the status of *p53* (Figures 3A and 3B). Remarkably, H3K9me3 and HP1γ immunofluorescence signals were absent in *p21* null mesonephric tubules and endolymphatic sac, whereas in WT embryos, most of the cells positive for H3K9me3 and HP1γ were also positive for p21 (Figures 3C and 3D). Moreover, in WT embryos, the levels of p21 increased progressively at both structures from E11.5 to E14.5 (Figure S2D), in a manner similar to that of the SAβG activity (Figures 1B and 1C).

We also explored the possible role of the DNA-damage-signaling kinases ATM and ATR, which induce senescence by activating p53 (Halazonetis et al., 2008; Toledo et al., 2008). For this, we examined the mesonephros and endolymphatic sac of *Atm* null embryos and *Atr*-Seckel embryos (the latter having a severe, but viable, reduction in *Atr* activity). However, none of them showed alterations in SAβG activity (Figure S3A), which is in agreement with the absence of detectable DNA damage in the senescent mesonephros and endolymphatic sac (see Figure S1E). Aside from DNA-damage signaling, p19ARF is another main activator of p53 (Collado et al., 2007). Thus, we examined *p16/p19ARF* null mice (Figure S3B) and also double-transgenic mice carrying one extra gene copy of the *p15/p16/p19ARF* locus and one extra gene copy of *p53* (Figure S3C). However, none of these embryos presented alterations in SAβG activity or Ki67 staining in the mesonephros or endolymphatic sac. These observations discard a role for p19ARF and p16 and are in agreement with their negative staining (see Figure S2A). The INK4 family of cell-cycle inhibitors (which includes $p16^{INK4a}$, $p15^{INK4b}$, $p18^{INK4c}$, and $p19^{INK4d}$) induces cell-cycle arrest by binding and inhibiting the cell-cycle kinases CDK4 and CDK6. To test the role of the INK4/CDK4,6 pathway, we analyzed mice carrying homozygous point mutations in CDK4 (mutation R24C) and CDK6 (mutation R31C) that prevent their binding to all the INK4 family members, thereby rendering them insensitive to these cell-cycle inhibitors. However, embryos *Cdk4-R24C*;*Cdk6-R31C* presented normal levels of SAβG activity and absence of Ki67 in the mesonephros and endolymphatic sac (Figure S3D). Finally, we also observed that *p27* null embryos presented normal levels of SAβG activity and Ki67-negative cells in both structures (Figure S3E).

To extend the concept of programmed senescence to human development, we examined human embryo samples at a stage when the mesonephros is regressing (16–17 mm crown-rump length, ~9 weeks pregnancy). Interestingly, the mesonephric tubules were negative for Ki67 and strongly positive for p21, whereas the Mullerian duct (an external duct attached to the mesonephros) and the definitive kidney tubules were positive for Ki67 and weak or negative for p21 (Figure 3E). A similar situation was encountered in the endolymphatic sac, with few Ki67-positive cells and abundant p21-positive cells (Figure 3F).

We conclude that developmentally programmed senescence in the mesonephros and endolymphatic sac is mediated by p21 in a p53-independent manner. Moreover, we exclude a relevant role for the DNA-damage-signaling kinases ATM and ATR, the p53 activator p19ARF, the p16 and p15 cell-cycle inhibitors, and, more generally, the INK4/CDK4,6 pathway, and we also exclude the cell-cycle inhibitor p27. Finally, we provide evidence for senescence features in the human mesonephros and endolymphatic sac.

Role of the TGF-β/SMAD Pathway in Developmentally Programmed Senescence

To gain insight into the pathways that could regulate senescence during development, we microdissected the mesonephric tubules of WT (n = 5) and *p21* null (n = 3) embryos at E14.5, and the obtained RNA was used to hybridize DNA microarrays. Analysis of the results with gene set enrichment analysis (GSEA) revealed that *p21* null mesonephric tubules have significantly

Figure 3. Developmentally Programmed Senescence at the Mesonephric Tubules and Endolymphatic Sac Depends on p21

(A) Mesonephric tubules of E14.5 murine embryos of the indicated genotypes stained for SAβG and, subsequently, counterstained with nuclear fast red (NFR), subjected to staining of Ki67 (left and central panels), or stained only for p21 (right panels), as indicated. The graphs show the percentage of blue surface, Ki67-positive cells, and p21-positive cells in the epithelia.

(B) Endolymphatic sacs stained and quantified as in (A).

(C) Mesonephric tubules at E14.5 stained for p21 (green), trimethylated lysine 9 of histone 3 (H3K9m3) (red), or HP1γ (red), as indicated. Nuclei were stained with DAPI (blue).

(D) Endolymphatic sacs stained as in (C).

(E) Human embryos (~9 weeks into pregnancy, n = 2) were stained for Ki67 and p21. Left panels show the entire mesonephros. The three small panels on the right show details. MD, Mullerian duct; WD, Wolffian duct; MT, mesonephric tubules.

(F) Human endolymphatic sac stained as in (E). Closed and open arrowheads indicate negative and positive nuclei, respectively, for p21.

Values are expressed as mean ± SD; the total number of embryos analyzed is indicated (n). Statistical significance relative to WT embryos was assessed by the two-tailed Student's t test: $^{**}p < 0.01$; $^{***}p < 0.001$.

See also Figure S3.

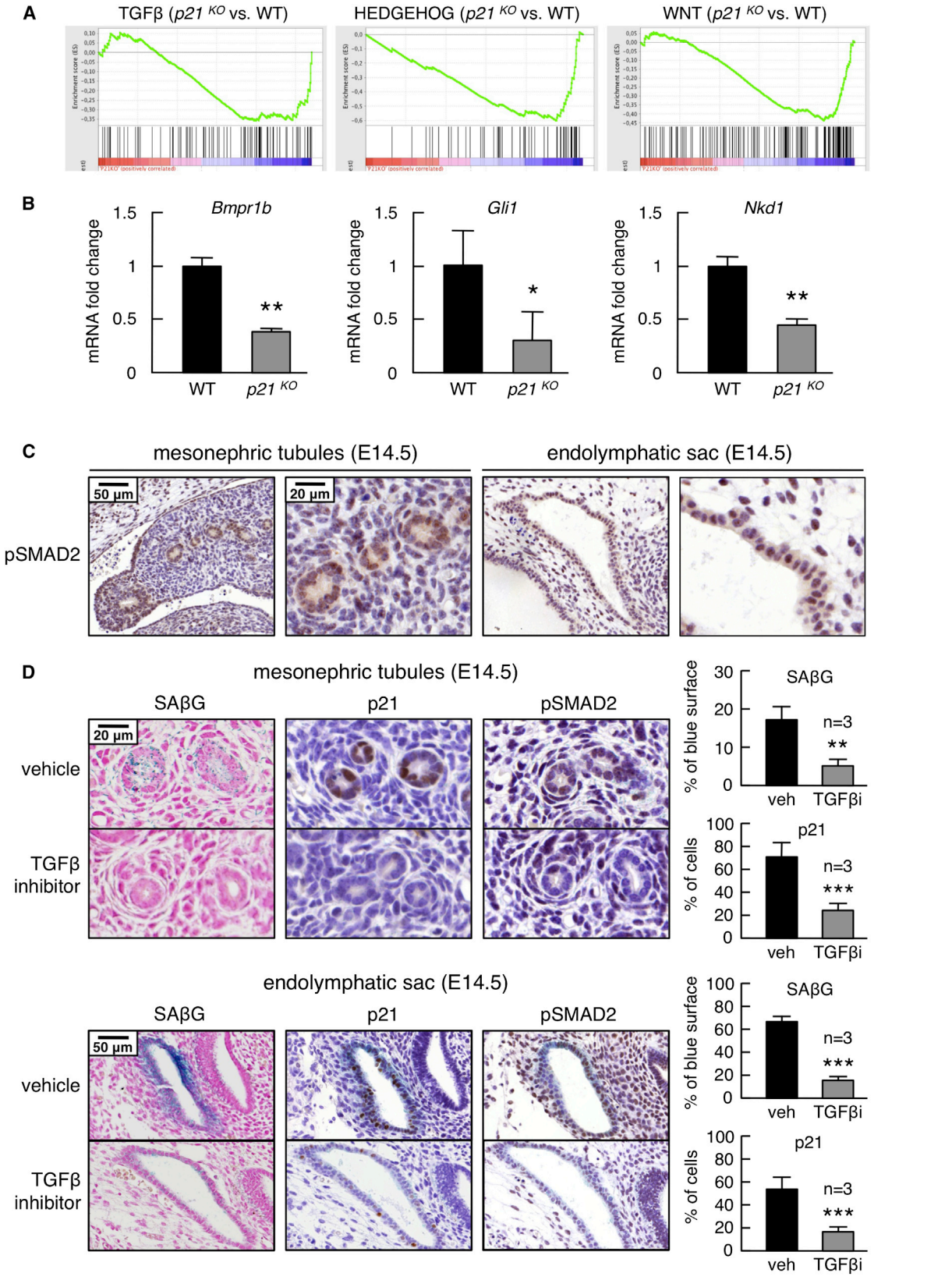

(legend on next page)

upregulated a number of pathways related to proliferation and DNA replication (Figure S4A and Table S2). On the other hand, important developmental pathways, such as the TGF-β, Hedgehog, and WNT pathways, were associated with WT tubules (i.e., senescent) and decreased in *p21* null tubules (i.e., nonsenescent) (Table S3; Figure 4A). Based on the most differentially expressed genes (Figure S4B and Tables S4 and S5), we confirmed by quantitative RT-PCR (qRT-PCR) that genes from these pathways are expressed at higher levels in WT tubules compared to *p21* null ones, including *Bmpr1b* (encoding the BMP receptor type 1B from the TGF-β pathway), *Gli1* (encoding a main transcription factor mediating the Hedgehog pathway), and *Nkd1* (encoding a regulator of the WNT pathway) (Figure 4B). The differential expression of *Gli1* was also confirmed by immunohistochemistry against GLI1 (Figure S4C). Of note, we could not detect statistically significant similarities between the global gene-expression profile of the senescent mesonephric epithelium and previously published gene-expression signatures of senescent fibroblasts induced by the infliction of DNA damage (Lafferty-Whyte et al., 2010), replicative senescence (Kim et al., 2013; Shelton et al., 1999), oncogene-induced senescence (Collado et al., 2005; Kuilman et al., 2008), or activation of tumor suppressors (Abad et al., 2007; Rovillain et al., 2011). Although different at a global gene-expression level, senescence in mesonephric epithelial cells and in fibroblasts share a subset of gene-expression changes. Most notably, the TGF-β pathway is commonly upregulated in the senescent mesonephros and in many types of damage/stress-induced senescence (Acosta et al., 2013; Kuilman and Peeper, 2009).

Based on these data, we investigated the possible functional association of the TGF-β pathway with p21-mediated developmentally programmed senescence. In particular, TGF-β activates the transcription of the *p21* gene through SMAD complexes (Datto et al., 1995; Nakae et al., 2003; Reynisdóttir et al., 1995). In support of this, we detected phosphorylated SMAD2 (i.e., active and nuclear) in the nuclei of the epithelial cells from the mesonephric tubules and the endolymphatic sac (Figure 4C). To causally connect the TGF-β pathway with senescence, we treated pregnant mice with a TGF-β pathway inhibitor (LY2152799), selective for the main TGF-β receptor, namely TGFBR1 or ALK5, by daily oral gavage from E10.5 to E14.5. As a control, phospho-SMAD2 was substantially decreased upon treatment with the TGF-β receptor inhibitor (Figure 4D). Remarkably, SAβG activity in the mesonephros and endolymphatic sac was quantitatively reduced after treatment with the TGF-β receptor inhibitor, and this was accompanied by a detectable reduction in p21 (Figure 4D). We conclude that p21-mediated developmentally programmed senescence is causally linked to the TGF-β/SMAD pathway.

Role of the PI3K/FOXO Pathway in Developmentally Programmed Senescence

We took note of the fact that FOXO proteins and SMAD proteins form complexes that bind and activate the *p21* promoter (Seoane et al., 2004). Based on this, we hypothesized that the PI3K/FOXO pathway (Greer and Brunet, 2005) could also participate in the regulation of developmentally programmed senescence. Specifically, staining for total FOXO1 revealed a mixture of positive and negative nuclei in the endolymphatic sac at E14.5 (Figure 5A), and we wondered whether this could be related to the heterogeneous pattern of p21-positive and -negative cells characteristic of this structure (see Figures 2B and S2D). To address this, we performed double immunofluorescence against p21 and phosphorylated FOXO1/3 (i.e., inactive and cytoplasmic). Interestingly, cells with high levels of pFOXO1/3 presented low levels of p21, and conversely, high levels of p21 were associated with low levels of pFOXO1/3 (Figures 5A and 5B). These results are compatible with FOXO1/3 being a positive regulator of p21 in the endolymphatic sac.

To validate the implication of the PI3K/FOXO pathway, we manipulated PI3K activity both genetically and chemically. We first analyzed *Pten*-transgenic mice (ubiquitously expressing about 2-fold levels of PTEN compared to WT mice). Interestingly, SAβG activity was increased in the mesonephros and endolymphatic sac of *Pten*-transgenic embryos (Figure 5C), and phosphorylated AKT levels were reduced (Figure 5C). The number of p21-positive cells was not significantly affected in *Pten*-transgenic embryos (Figure S5A), suggesting that the reinforcement of senescence might be due to an increase in the levels of p21 within senescent cells, rather than to an increase in the number of p21-positive cells. As an additional proof, we used a potent small compound inhibitor of PI3K, namely CNIO-PI3Ki, which is highly specific for PI3K catalytic subunits p110α and p110δ (Ortega-Molina et al., 2012). The compound was administered by daily oral gavage to pregnant females from E10.5 to E14.5. Interestingly, exposure to CNIO-PI3Ki produced a remarkable quantitative increase in the SAβG signal in the mesonephric tubules and endolymphatic sac (Figures 5D and 5E). As in the case of *Pten*-transgenic mice, this treatment was accompanied by a decrease in pAKT (Figure 5D) and did not affect the number of p21-positive cells (Figure S5B).

In addition to FOXO activation, low PI3K activity also results in mTOR downregulation (Zoncu et al., 2011). To explore the

Figure 4. Developmentally Programmed Senescence Is Associated with the TGF-β Pathway

(A) GSEA plots of *p21* null (n = 3) compared to WT (n = 5) microdissected mesonephric tubules for the indicated gene sets.

(B) Expression of the indicated genes by qRT-PCR in mesonephric tubules of WT (n = 3) or *p21* null (n = 3) embryos.

(C) Staining of phosphorylated SMAD2 in the mesonephric tubules (left) and the endolymphatic sac (right) of WT embryos. At least five embryos were stained, obtaining similar results.

(D) Mesonephric tubules and endolymphatic sac of embryos from pregnant WT females daily treated with vehicle or with a TGF-β inhibitor (LY2157299) from E10.5 to E14.5. Embryos were subjected to whole-mount SAβG staining and then counterstained with NFR or subjected to immunohistochemical staining of p21 or pSMAD2. The graphs show the percentage of blue surface and p21-positive cells in the mesonephric tubules and the endolymphatic sac. These results were obtained in a total of three embryos per condition, each from a separate pregnancy.

All samples correspond to embryos at E14.5. Values are expressed as mean ± SD. Statistical significance was assessed by the two-tailed Student's t test: *$p < 0.05$; **$p < 0.01$; ***$p < 0.001$.

See also Figure S4 and Tables S2, S3, S4, and S5.

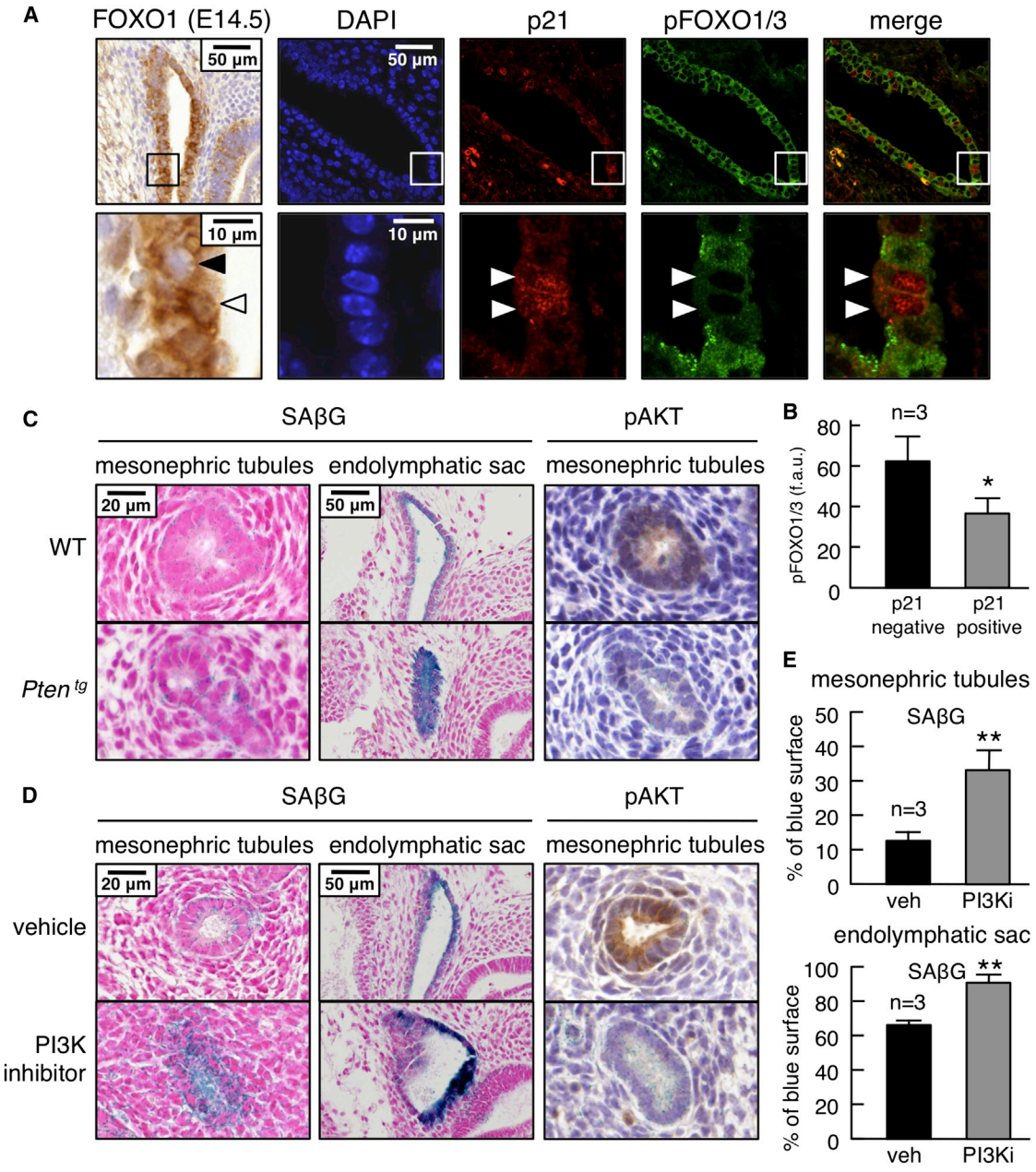

Figure 5. Inhibition of PI3K Enhances Developmentally Programmed Senescence

(A) Endolymphatic sacs of WT embryos stained for total FOXO1 and for p21 (red), pFOXO1/3 (green), and DAPI (blue). In the case of FOXO1, the black arrowhead indicates a negative nucleus, and the white arrowhead a positive one; in the other panels, white arrowheads indicate p21-positive and pFOXO1/3-negative nuclei.

(B) Quantification of pFOXO1/3 detected by immunofluorescence, as in (A), and measured as fluorescence arbitrary units (f.a.u.).

(C) Mesonephric tubules and endolymphatic sacs of embryos of the indicated genotypes stained for SAβG. The mesonephric tubules were subsequently stained for phosphorylated AKT.

(D) Mesonephric tubules and endolymphatic sacs of embryos from pregnant females daily treated with vehicle or with a PI3K inhibitor (CNIO-PI3Ki), from E10.5 to E14.5, and stained for SAβG. The mesonephric tubules were subsequently stained for phosphorylated AKT.

(E) Percentage of blue surface in SAβG staining as in (D).

All samples correspond to E14.5 embryos at the indicated conditions or genotypes. Equivalent results were obtained in a total of three embryos per condition or genotype, each from a separate pregnancy. Values are expressed as mean ± SD. Statistical significance was assessed by the two-tailed Student's t test: *$p < 0.05$; **$p < 0.01$.

See also Figure S5.

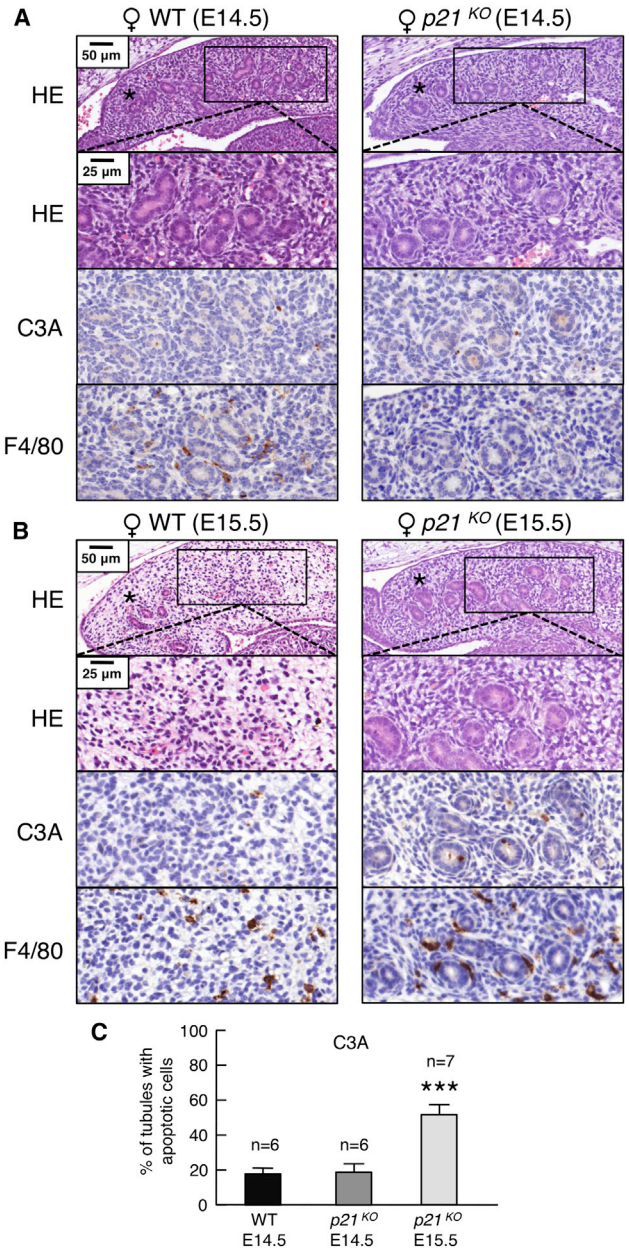

Figure 6. Delayed Mesonephric Regression in *p21* Null Mice

(A) Histological sections stained with hematoxylin and eosin (H&E), active caspase-3 (C3A), and EGF-like module-containing mucin-like hormone receptor-like 1 (F4/80) of the mesonephros of WT and *p21* null female embryos at E14.5. Asterisks indicate the apical tubular area, and rectangles indicate the caudal tubular area. The bottom panels show a magnification of the caudal tubular areas. Equivalent results were obtained in a total of three embryos per genotype.

(B) Same as (A) but at E15.5.

(C) Percentage of mesonephric tubules with at least one C3A-positive cell at the indicated times and genotypes. Values are expressed as mean ± SD at the indicated number of embryos (n). Statistical significance relative to WT E14.5 tubules was assessed by the two-tailed Student's t test: ***$p < 0.001$.

See also Figure S6.

putative relevance of mTOR, we treated pregnant females with rapamycin under conditions that decreased phosphorylated S6 protein in the embryo (Hirota et al., 2011). However, SAβG activity in the mesonephric tubules and endolymphatic sac was similar between rapamycin-treated and vehicle-treated embryos (Figure S5C), thus suggesting that mTOR downregulation is not an important mediator of developmental senescence. Finally, the levels of pSMAD2 and FOXO1 increased from E11.5 to E14.5, thus following the same pattern as p21 and SAβG (Figure S5D; see Figures 1C, 2B, and S2D).

In summary, through a combination of genetic and chemical approaches, we conclude that the TGF-β/SMAD and PI3K/FOXO pathways directly participate in developmentally programmed senescence.

Clearance of Senescent Cells and Partial Compensatory Mechanisms in *p21* Null Mice

Senescent cells can be efficiently cleared through macrophage-mediated phagocytosis (Kang et al., 2011; Xue et al., 2007), and macrophages are known to infiltrate the regressing mesonephros (Camp and Martin, 1996). We observed abundant macrophages surrounding senescent mesonephric tubules at E14.5 (Figures 6A and S6A). However, macrophages were absent at E12.5 (Figure S6A), a developmental stage when mesonephric tubules are already senescent according to SAβG, p21, and Ki67 levels (see Figures 1B and 2A). This is consistent with the idea that senescence precedes macrophage infiltration. We also considered the possible contribution of apoptosis to the regression of the mesonephric tubules. At E14.5, most of the mesonephric tubules were free of apoptotic cells, although surrounded by macrophages (Figure 6A). Later, at days E15.5 and E16.5, caudal tubules had disappeared, and macrophages remained abundant (Figures 6B, S6B, and S6C). We conclude that cells undergoing developmentally programmed senescence are cleared by macrophages in the absence of widespread apoptosis.

We wondered about the fate of the mesonephric tubules when developmental senescence is genetically ablated. Interestingly, the mesonephros of *p21* null embryos presented minimal macrophage infiltration at E14.5 (Figure 6A) and did not present increased apoptosis compared to WT mesonephros (Figures 6A and 6C). However, this situation changed on the following day (E15.5), when apoptosis was significantly increased in the *p21* null tubules (Figure 6C) and the mesonephros became massively infiltrated by macrophages surrounding the caudal tubules (Figures 6B and S6B). It should be noted that at this time, the caudal tubules of the WT mesonephros have already disappeared, thus indicating a delayed regression of the *p21* null mesonephros. At day E16.5, the mesonephric remnants of WT and *p21* null embryos were similar, lacking caudal tubules and still being heavily infiltrated by macrophages (Figure S6C). Therefore, the absence of senescence in *p21* null mesonephric tubules is compensated by a delayed activation of an apoptotic program that is followed by macrophage-mediated clearance.

A similar analysis was performed in the endolymphatic sac. Interestingly, *p21* null embryos at a late stage of development (E18.5) had a remarkably abnormal endolymphatic sac with multiple infoldings that crossed and filled most of the lumen of the sac (Figure S7A). However, this defect was ameliorated in

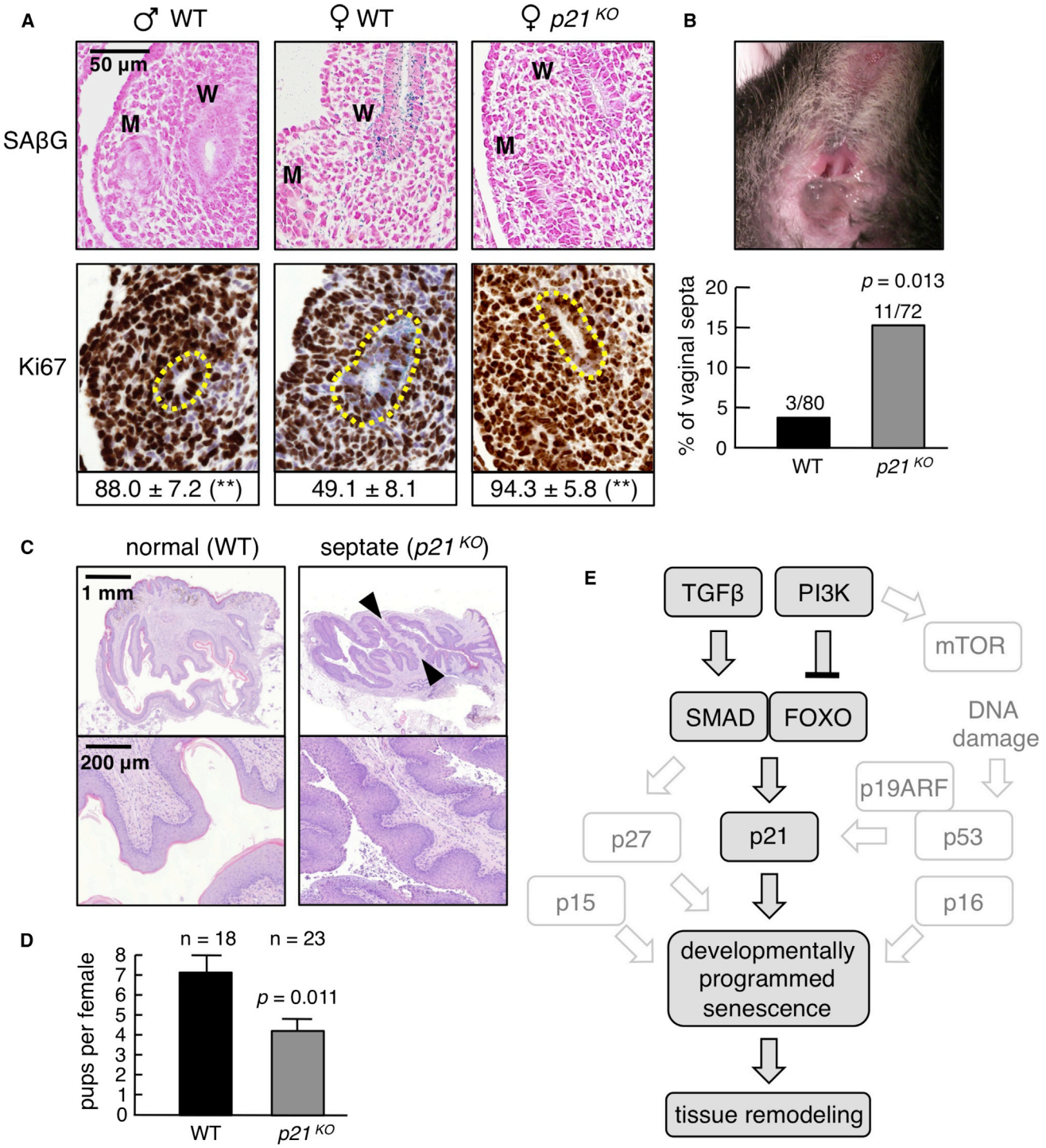

Figure 7. Developmentally Programmed Senescence in the Female Wolffian Duct and Morphologic Abnormalities in the Vaginas of *p21* Null Mice

(A) Wolffian (W) and Mullerian (M) ducts at the caudal ends of the mesonephros in male or female E14.5 embryos of the indicated genotypes stained for SAβG or Ki67, as indicated. The percentage of Ki67-positive cells in the Wolffian duct epithelium at the caudal mesonephric region is shown. In the case of WT females and males, n = 4 per sex; in the case of *p21* null females, n = 3. Values are expressed as mean ± SD. Statistical significance relative to WT female was assessed by the two-tailed Student's t test: **p < 0.01.

(B) External view of a septate vagina and graph with the percentages of septate vagina in WT and *p21* null female littermates. The number of septate vaginas and the total number of females examined are indicated. Statistical significance was assessed by the Fisher's exact test.

(legend continued on next page)

newborns (E19.5/postnatal day 0 [P0]) (Figure S7A), and it was undetectable in adult mice (Figure S7B). In agreement with the normalization of the endolymphatic sac, extensive hearing and balance tests did not reveal detectable functional defects in adult *p21* null mice (Figure S7C and Table S6).

Previous investigators have reported that a minor population of cells from the endolymphatic sac undergo a robust expansion after E14.5 (Kim and Wangemann, 2011). These cells are characterized by the expression of pendrin, an anion transporter, also known as SLC26A4, important for the outflow of the endolymph at the sac of the inner ear. We hypothesized that the role of senescence at the endolymphatic sac is to arrest the major population of cells present at E14.5 in favor of the minor pendrin-positive population. Indeed, we observed a lack of colocalization of p21-positive cells and pendrin-positive cells, indicating that they constitute different cell populations (Figure S7D). Interestingly, at E18.5, pendrin-positive cells were underrepresented in *p21* null embryos compared to WT (Figure S7E). These observations suggest that an important biological function of senescence at the endolymphatic sac is to regulate the balance between different cell populations.

Finally, we asked about the mechanisms that correct the aberrant morphology of the *p21* null endolymphatic sac at perinatal stages. For this, we stained E18.5 embryos and E19.5/P0 perinatal mice for SAβG, caspase-3 (C3A), and macrophages (F4/80) (Figure S7F). Most of the infoldings present in *p21* null sacs, and to a lower extent in WT sacs, had apoptotic cells and macrophage infiltration in the absence of senescence (Figure S7F). We interpret that the elimination of endolymphatic sac infoldings, both in WT and *p21* null embryos, is a macrophage-dependent remodeling process that occurs during late development independently of senescence.

In summary, we conclude that developmentally programmed senescence can play at least two roles: elimination of structures through macrophage-dependent clearance, as in the case of the mesonephric tubules, and determination of the balance between cell populations, as in the case of the endolymphatic sac. In the absence of developmentally programmed senescence, compensatory mechanisms can correct these defective morphogenic processes, either by apoptosis, as observed in the mesonephros, or through a general remodeling mediated by macrophages, as observed in the endolymphatic sac.

Morphological Abnormalities in *p21* Null Mice

In the case of the mesonephros, the only structure that does not undergo complete regression is the Wolffian duct. Specifically, in the case of males, the Wolffian duct proliferates and differentiates into the epididymis and the vas deferens (Davidson, 2008). In contrast, most of the female Wolffian duct degenerates, with the notable exception of the caudal portion that participates in the formation of the vagina (Kurita, 2010; Orvis and Behringer, 2007). Importantly, the different behavior of the Wolffian duct in males (expansion) and females (partial regression) correlated with senescence at E14.5 (Figure 7A). In the case of males, hardly any SAβG activity was present in the Wolffian duct at the caudal mesonephros, whereas SAβG was present in the female Wolffian duct. Also, the male Wolffian duct had a higher percentage of Ki67-positive cells compared to the female Wolffian duct (Figure 7A). In line with our previous findings, senescence was dependent on p21, as inferred by the absence of SAβG activity and high Ki67 levels in the Wolffian duct of *p21* null females (Figure 7A). These results demonstrate that p21-dependent senescence occurs specifically in the female, but not in the male, Wolffian duct.

We wondered whether the absence of senescence in *p21* null females had an impact on the morphogenesis of the vagina. Interestingly, we observed that up to 15% of the adult *p21* null females had a visible dorsoventral vaginal septum (Figure 7B). Septate vaginas were confirmed by histology (Figure 7C) and by ultrasound imaging (Movies S1 and S2). These septa were also found in a small percentage of WT females (3.75%), which is in agreement with a previous report on the incidence of septate vagina in laboratory mice (Cunliffe-Beamer and Feldman, 1976). Vaginal septa are known to reduce fertility, due in part to mucus accumulation and associated infectious processes that may affect the viability of the fetuses (Lezmi et al., 2011). Indeed, *p21* null females had a lower number of pups compared to WT females (Figure 7D). Together, these results indicate that defective programmed senescence in the Wolffian duct of *p21* null females results in an increased incidence of vaginal septa, thus compromising fertility.

DISCUSSION

Essential Role of p21 in Developmentally Programmed Senescence

Here, we report that cellular senescence occurs at multiple locations during mammalian embryonic development. We have analyzed in detail the biological mechanisms and developmental significance of senescence in the regressing mesonephros and in the endolymphatic sac of the inner ear. Developmentally programmed senescence in these structures was defined by the presence of SAβG activity, heterochromatin markers (H3K9me3, HP1γ), and proliferative arrest (exclusion of Ki67). A number of senescence effectors were found expressed in the mesonephros and endolymphatic sac, namely p53, p21, p27, and p15. However, extensive genetic analyses indicated that only p21 was critical for developmental senescence at the studied structures (Figure 7E). Also, we could not detect evidence for DNA-damage markers in the senescent cells of the mesonephros and endolymphatic sac, nor an involvement of the DNA-damage-signaling kinases ATM or ATR. Therefore, developmentally

(C) Histological analyses of transversal sections of normal and septate vaginas from adult females of the indicated genotypes. Arrowheads point to the vaginal septum.

(D) Mean number of pups per female of the indicated genotypes. The total number of litters examined is indicated. Values are expressed as mean ± SD, and statistical significance was assessed by the two-tailed Student's t test.

(E) Summary of the molecular mechanisms regulating developmentally programmed senescence.

See also Figure S7, Table S6, and Movies S1 and S2.

programmed senescence is characterized by its dependency on p21 and by the absence of obvious damage signals.

Signaling Pathways Regulating Developmentally Programmed Senescence

Gene-expression analysis in the mesonephros suggested the upregulation of the TGF-β, Hedgehog, and WNT pathways in developmental senescence. We focused on the TGF-β pathway because of its previous involvement in senescence (Acosta et al., 2013; Kuilman and Peeper, 2009) and its well-established capacity to activate the transcription of the *p21* gene through SMAD complexes (Datto et al., 1995; Nakae et al., 2003; Reynisdóttir et al., 1995). We found high levels of phospho-SMAD2 (i.e., active) in the epithelia of the mesonephros and endolymphatic sac. Interestingly, treatment of pregnant females with a TGF-β pathway inhibitor significantly reduced SAβG activity and p21 levels, thus demonstrating a direct impact of the TGF-β pathway on p21-mediated senescence. TGF-β-activated SMAD proteins are known to act in concert with FOXO proteins (Seoane et al., 2004) and, based on this, we examined the impact of the PI3K/FOXO pathway on p21-mediated senescence. In particular, genetic overexpression of *Pten*, which is a positive regulator of FOXO through inhibition of PI3K, and treatment of pregnant females with a PI3K inhibitor resulted in stronger senescence at the mesonephros and endolymphatic sac. Altogether, we conclude that the TGF-β/SMAD and PI3K/FOXO pathways are involved in p21-mediated developmentally programmed senescence (Figure 7E).

We find it remarkable that two separate developmental processes share not only the same critical effector, namely p21, but also the same regulatory pathways. Based on this, it is tempting to speculate that these mechanisms could be common to other processes of developmental senescence. In this regard, it is important to mention that the accompanying paper shows that p21 has been also involved in senescence during neural tube closure and digit formation (Storer et al., 2013).

Clearance of Senescent Cells and Compensatory Mechanisms

Emerging evidence indicates that tumoral cells that undergo damage-induced senescence are ultimately cleared by macrophages (Kang et al., 2011; Xue et al., 2007). Interestingly, we observed that macrophages infiltrate and surround the senescent mesonephric tubules, which are efficiently eliminated at day E15.5. The recruitment of macrophages by senescent cells is a complex process incompletely understood (Hoenicke and Zender, 2012), where TGF-β plays a relevant role (Flavell et al., 2010). In contrast, senescence is absent and macrophage infiltration is negligible in *p21* null embryos at E14.5. A day later, the mesonephric tubules of WT embryos have disappeared, whereas those of *p21* null remain essentially intact. Nonetheless, *p21* null tubules are efficiently eliminated by E16.5 through a compensatory process that involves apoptosis and massive macrophage infiltration. Therefore, in the case of the mesonephros, senescence behaves as the primary signal that triggers macrophage-mediated elimination, but, if senescence fails, a delayed apoptotic program can also accomplish mesonephric involution.

The endolymphatic sac, in contrast to the mesonephros, is not eliminated during development, but it undergoes a process of differential arrest and expansion of selective cell populations. This is exemplified by the expansion of pendrin-positive cells that occurs after E14.5 (Kim and Wangemann, 2011). In the case of *p21* null embryos, the endolymphatic sac presents an abnormal expansion of pendrin-negative cells presumably as a consequence of the lack of senescence. This unbalanced cell ratio is accompanied by numerous aberrant infoldings that fill the lumen of the sac. However, at late stages of development, the few papillae present in WT sacs, as well as the numerous ones in *p21* null sacs, undergo a general process of elimination associated with macrophage infiltration independently of senescence. Therefore, we conclude that the biological function of senescence at the endolymphatic sac is to establish a correct balance between cell populations.

The observation that other processes can compensate deficient senescence is not surprising given the robustness of embryonic development. In relation to this, for example, severe disabling of apoptosis results in relatively minor developmental defects, restricted to imperforate vaginas and a partial persistence of interdigital webs (Lindsten et al., 2000; Ren et al., 2010). Curiously, the formation of the vagina and the digits are two morphogenic processes that involve senescence (our current work; Storer et al., 2013). This could reflect a more general trend whereby senescence and apoptosis are mutually compensatory and interconnected during developmental processes.

Developmental Defects Associated with Impaired Programmed Senescence

Despite the compensatory processes mentioned above, we wondered whether the failure to undergo senescence could affect adult structures. We observed that the female Wolffian duct is almost completely eliminated during normal development except for its contribution to the caudal region of the vagina (Kurita, 2010; Orvis and Behringer, 2007). This is in contrast to the male Wolffian duct that expands and differentiates into the vas deferens and epididymis. Notably, during mesonephric involution, the female Wolffian duct undergoes p21-mediated senescence, whereas the male Wolffian duct remains proliferative. We examined the vaginas of adult *p21* null females and found a remarkable incidence of septa, which is consistent with an abnormal contribution of the Wolffian ducts to the formation of the vagina, and this was accompanied by a reduced fertility. Therefore, at least in the case of the mesonephros and its derived structures, compensatory processes do not fully replace the absence of developmentally programmed senescence. We anticipate the existence of other mediators of senescence that, together with p21, may contribute to developmental senescence, and their combined inactivation may result in more severe morphogenic defects.

Concluding Remarks

In summary, our findings expand the biology of cellular senescence from stress responses associated with pathological states, cancer, and aging to morphological processes during embryonic development in mammals. Developmentally programmed senescence is a physiological process that occurs

predictably and reproducibly in response to developmental cues, whereas, in contrast, damage/stress-induced senescence is triggered by nonphysiological insults or pathological states. We have focused on two developmental processes associated with senescence, and interestingly, both of them shared the same mechanistic principles, including the implication of the TGF-β/SMAD and PI3K/FOXO pathways and the critical role of p21. Importantly, senescence features are also present in human embryos.

Conceptually, we add cellular senescence to the collection of processes that contribute to embryonic development, together with proliferation, differentiation, migration, and cell death. This opens up the possibility that cellular senescence originated in evolution as a tissue-remodeling mechanism during embryonic development, and it was subsequently adapted to orchestrate tissue regeneration and healing upon damage in adult organisms.

EXPERIMENTAL PROCEDURES

Mice

All animal procedures were performed according to protocols approved by the CNIO-ISCIII Ethics Committee for Research and Animal Welfare (CElyBA).

Human Samples

Human embryos were obtained by A.R.-B. from spontaneous abortions voluntarily donated by the mother to hospitals affiliated with the Universitat Autònoma de Barcelona, under signed informed consent following the ethical procedures of the corresponding hospitals.

Treatment with Chemical Inhibitors

Pregnant females were treated by daily oral gavage, from days E10.5 to E14.5, with the following compounds: LY2157299 (25 mg/kg) (Axon MedChem); CNIO-PI3Ki (15 mg/kg) (Ortega-Molina et al., 2012); and rapamycin (20 mg/kg) (LC laboratories). Mice were sacrificed 6 hr after the last dose and processed for histological analyses. For additional details, see the Extended Experimental Procedures.

Statistical Analyses

All quantitative data are presented as mean ± SD. Two-tailed Student's t test was carried out to assess statistical significance, unless otherwise indicated.

Accesion Numbers

The microarray data have been deposited in the Gene Expression Omnibus (GEO) database (http://www.ncbi.nlm.nih.gov/geo/) under the accession number GSE49108.

SUPPLEMENTAL INFORMATION

Supplemental Information includes Extended Experimental Procedures, seven figures, six tables, and two movies and can be found with this article online at http://dx.doi.org/10.1016/j.cell.2013.10.019.

AUTHOR CONTRIBUTIONS

D.M.-E. performed most of the experiments, contributed to the experimental design, data analysis, discussion, and writing of the paper; M. Cañamero performed most of the histological analyses and contributed to data analysis. A.M. performed some experiments, including microdissection, RNA extraction, microarray analysis, and validation, and contributed to data analysis. G.G.-L. performed the biocomputing analyses. J.C. helped with the histological analyses of the inner ear; S.M.-C. performed the hearing and balance tests. A.R.-B. obtained the human embryo samples. I.V.-N. designed, supervised, and interpreted the analyses of the inner ear. J.R. contributed to the interpretation of the data on the mesonephros and vagina. M. Collado contributed to the experimental design, data analysis, and discussion. M.S. designed and supervised the study, secured funding, analyzed the data, and wrote the manuscript. All authors discussed the results and commented on the manuscript.

ACKNOWLEDGMENTS

We thank Marcos Malumbres, Oscar Fernández-Capetillo, Mirna Pérez-Moreno, and Donatello Castellano for sharing critical reagents. We also thank for excellent technical support the CNIO Genomics, Animal Facility, Histopathology, Confocal Microscopy, and Molecular Imaging Units. D.M.-E. has been funded by the Juan de la Cierva Program. A.M. and M. Collado were funded by the Miguel Servet Program. S.M.-C. holds a CIBERER (ISCIII) postdoctoral contract. Work in the laboratory of M.S. is funded by the CNIO and by grants from the MICINN (SAF), the Regional Government of Madrid, the European Research Council (Advanced ERC Grant), the Botín Foundation, the Ramón Areces Foundation, and the AXA Foundation. Work in the I.V.-N. group is supported by grants from MINECO (SAF2011-24391), Fundación de Investigación Médica Mutua Madrileña (2012), and AFHELO (FP7, European Union).

Received: February 11, 2013
Revised: July 19, 2013
Accepted: October 12, 2013
Published: November 14, 2013

REFERENCES

Abad, M., Menéndez, C., Füchtbauer, A., Serrano, M., Füchtbauer, E.M., and Palmero, I. (2007). Ing1 mediates p53 accumulation and chromatin modification in response to oncogenic stress. J. Biol. Chem. *282*, 31060–31067.

Acosta, J.C., Banito, A., Wuestefeld, T., Georgilis, A., Janich, P., Morton, J.P., Athineos, D., Kang, T.W., Lasitschka, F., Andrulis, M., et al. (2013). A complex secretory program orchestrated by the inflammasome controls paracrine senescence. Nat. Cell Biol. *15*, 978–990.

Camp, V., and Martin, P. (1996). The role of macrophages in clearing programmed cell death in the developing kidney. Anat. Embryol. (Berl.) *194*, 341–348.

Campisi, J., and d'Adda di Fagagna, F. (2007). Cellular senescence: when bad things happen to good cells. Nat. Rev. Mol. Cell Biol. *8*, 729–740.

Collado, M., and Serrano, M. (2006). The power and the promise of oncogene-induced senescence markers. Nat. Rev. Cancer *6*, 472–476.

Collado, M., and Serrano, M. (2010). Senescence in tumours: evidence from mice and humans. Nat. Rev. Cancer *10*, 51–57.

Collado, M., Blasco, M.A., and Serrano, M. (2007). Cellular senescence in cancer and aging. Cell *130*, 223–233.

Collado, M., Gil, J., Efeyan, A., Guerra, C., Schuhmacher, A.J., Barradas, M., Benguría, A., Zaballos, A., Flores, J.M., Barbacid, M., et al. (2005). Tumour biology: senescence in premalignant tumours. Nature *436*, 642.

Conradt, B. (2009). Genetic control of programmed cell death during animal development. Annu. Rev. Genet. *43*, 493–523.

Cunliffe-Beamer, T.L., and Feldman, D.B. (1976). Vaginal septa in mice: incidence, inheritance, and effect on reproductive, performance. Lab. Anim. Sci. *26*, 895–898.

Datto, M.B., Li, Y., Panus, J.F., Howe, D.J., Xiong, Y., and Wang, X.F. (1995). Transforming growth factor beta induces the cyclin-dependent kinase inhibitor p21 through a p53-independent mechanism. Proc. Natl. Acad. Sci. USA *92*, 5545–5549.

Davidson, A.J. (2008). Mouse kidney development. In StemBook (Harvard Stem Cell Institute). http://www.stembook.org/node/532.

Dimri, G.P., Lee, X., Basile, G., Acosta, M., Scott, G., Roskelley, C., Medrano, E.E., Linskens, M., Rubelj, I., Pereira-Smith, O., et al. (1995). A biomarker that identifies senescent human cells in culture and in aging skin in vivo. Proc. Natl. Acad. Sci. USA *92*, 9363–9367.

Flavell, R.A., Sanjabi, S., Wrzesinski, S.H., and Licona-Limón, P. (2010). The polarization of immune cells in the tumour environment by TGFbeta. Nat. Rev. Immunol. *10*, 554–567.

Freund, A., Orjalo, A.V., Desprez, P.Y., and Campisi, J. (2010). Inflammatory networks during cellular senescence: causes and consequences. Trends Mol. Med. *16*, 238–246.

Fuchs, Y., and Steller, H. (2011). Programmed cell death in animal development and disease. Cell *147*, 742–758.

Gorgoulis, V.G., and Halazonetis, T.D. (2010). Oncogene-induced senescence: the bright and dark side of the response. Curr. Opin. Cell Biol. *22*, 816–827.

Greer, E.L., and Brunet, A. (2005). FOXO transcription factors at the interface between longevity and tumor suppression. Oncogene *24*, 7410–7425.

Halazonetis, T.D., Gorgoulis, V.G., and Bartek, J. (2008). An oncogene-induced DNA damage model for cancer development. Science *319*, 1352–1355.

Hirota, Y., Cha, J., Yoshie, M., Daikoku, T., and Dey, S.K. (2011). Heightened uterine mammalian target of rapamycin complex 1 (mTORC1) signaling provokes preterm birth in mice. Proc. Natl. Acad. Sci. USA *108*, 18073–18078.

Hoenicke, L., and Zender, L. (2012). Immune surveillance of senescent cells—biological significance in cancer- and non-cancer pathologies. Carcinogenesis *33*, 1123–1126.

Hultcrantz, M., Bagger-Sjöbäck, D., and Rask-Andersen, H. (1987). The development of the endolymphatic duct and sac. A light microscopical study. Acta Otolaryngol. *104*, 406–416.

Kang, T.W., Yevsa, T., Woller, N., Hoenicke, L., Wuestefeld, T., Dauch, D., Hohmeyer, A., Gereke, M., Rudalska, R., Potapova, A., et al. (2011). Senescence surveillance of pre-malignant hepatocytes limits liver cancer development. Nature *479*, 547–551.

Kim, H.M., and Wangemann, P. (2011). Epithelial cell stretching and luminal acidification lead to a retarded development of stria vascularis and deafness in mice lacking pendrin. PLoS ONE *6*, e17949.

Kim, Y.M., Byun, H.O., Jee, B.A., Cho, H., Seo, Y.H., Kim, Y.S., Park, M.H., Chung, H.Y., Woo, H.G., and Yoon, G. (2013). Implications of time-series gene expression profiles of replicative senescence. Aging Cell *12*, 622–634.

Kourtis, N., and Tavernarakis, N. (2007). Non-developmentally programmed cell death in Caenorhabditis elegans. Semin. Cancer Biol. *17*, 122–133.

Krizhanovsky, V., Xue, W., Zender, L., Yon, M., Hernando, E., and Lowe, S.W. (2008). Implications of cellular senescence in tissue damage response, tumor suppression, and stem cell biology. Cold Spring Harb. Symp. Quant. Biol. *73*, 513–522.

Kuilman, T., and Peeper, D.S. (2009). Senescence-messaging secretome: SMS-ing cellular stress. Nat. Rev. Cancer *9*, 81–94.

Kuilman, T., Michaloglou, C., Vredeveld, L.C., Douma, S., van Doorn, R., Desmet, C.J., Aarden, L.A., Mooi, W.J., and Peeper, D.S. (2008). Oncogene-induced senescence relayed by an interleukin-dependent inflammatory network. Cell *133*, 1019–1031.

Kurita, T. (2010). Developmental origin of vaginal epithelium. Differentiation *80*, 99–105.

Kurz, D.J., Decary, S., Hong, Y., and Erusalimsky, J.D. (2000). Senescence-associated (beta)-galactosidase reflects an increase in lysosomal mass during replicative ageing of human endothelial cells. J. Cell Sci. *113*, 3613–3622.

Lafferty-Whyte, K., Bilsland, A., Cairney, C.J., Hanley, L., Jamieson, N.B., Zaffaroni, N., Oien, K.A., Burns, S., Roffey, J., Boyd, S.M., and Keith, W.N. (2010). Scoring of senescence signalling in multiple human tumour gene expression datasets, identification of a correlation between senescence score and drug toxicity in the NCI60 panel and a pro-inflammatory signature correlating with survival advantage in peritoneal mesothelioma. BMC Genomics *11*, 532.

Lezmi, S., Thibault-Duprey, K., Bidaut, A., Hardy, P., Pino, M., Macary, G.S., Barbellion, S., Brunel, P., Dorchies, O., Clifford, C., and Leconte, I. (2011). Spontaneous metritis related to the presence of vaginal septum in pregnant Sprague Dawley Crl:CD(SD) rats: impact on reproductive toxicity studies. Vet. Pathol. *48*, 964–969.

Lindsten, T., Ross, A.J., King, A., Zong, W.X., Rathmell, J.C., Shiels, H.A., Ulrich, E., Waymire, K.G., Mahar, P., Frauwirth, K., et al. (2000). The combined functions of proapoptotic Bcl-2 family members bak and bax are essential for normal development of multiple tissues. Mol. Cell *6*, 1389–1399.

Lo, W.W., Daniels, D.L., Chakeres, D.W., Linthicum, F.H., Jr., Ulmer, J.L., Mark, L.P., and Swartz, J.D. (1997). The endolymphatic duct and sac. AJNR Am. J. Neuroradiol. *18*, 881–887.

Nacher, V., Carretero, A., Navarro, M., Armengol, C., Llombart, C., Rodríguez, A., Herrero-Fresneda, I., Ayuso, E., and Ruberte, J. (2006). The quail mesonephros: a new model for renal senescence? J. Vasc. Res. *43*, 581–586.

Nakae, J., Kitamura, T., Kitamura, Y., Biggs, W.H., 3rd, Arden, K.C., and Accili, D. (2003). The forkhead transcription factor Foxo1 regulates adipocyte differentiation. Dev. Cell *4*, 119–129.

Narita, M., Nũnez, S., Heard, E., Narita, M., Lin, A.W., Hearn, S.A., Spector, D.L., Hannon, G.J., and Lowe, S.W. (2003). Rb-mediated heterochromatin formation and silencing of E2F target genes during cellular senescence. Cell *113*, 703–716.

Ortega-Molina, A., Efeyan, A., Lopez-Guadamillas, E., Muñoz-Martin, M., Gómez-López, G., Cañamero, M., Mulero, F., Pastor, J., Martinez, S., Romanos, E., et al. (2012). Pten positively regulates brown adipose function, energy expenditure, and longevity. Cell Metab. *15*, 382–394.

Orvis, G.D., and Behringer, R.R. (2007). Cellular mechanisms of Müllerian duct formation in the mouse. Dev. Biol. *306*, 493–504.

Ren, D., Tu, H.C., Kim, H., Wang, G.X., Bean, G.R., Takeuchi, O., Jeffers, J.R., Zambetti, G.P., Hsieh, J.J., and Cheng, E.H. (2010). BID, BIM, and PUMA are essential for activation of the BAX- and BAK-dependent cell death program. Science *330*, 1390–1393.

Reynisdóttir, I., Polyak, K., Iavarone, A., and Massagué, J. (1995). Kip/Cip and Ink4 Cdk inhibitors cooperate to induce cell cycle arrest in response to TGF-beta. Genes Dev. *9*, 1831–1845.

Rovillain, E., Mansfield, L., Caetano, C., Alvarez-Fernandez, M., Caballero, O.L., Medema, R.H., Hummerich, H., and Jat, P.S. (2011). Activation of nuclear factor-kappa B signalling promotes cellular senescence. Oncogene *30*, 2356–2366.

Sainio, K. (2003). Development of the mesonephric kidney. In The kidney. From normal development to congenital disease, C. Vize, A.S. Woolf, and J.B.L. Bard, eds. (London: Academic Press), pp. 75–86.

Seoane, J., Le, H.V., Shen, L., Anderson, S.A., and Massagué, J. (2004). Integration of Smad and forkhead pathways in the control of neuroepithelial and glioblastoma cell proliferation. Cell *117*, 211–223.

Shelton, D.N., Chang, E., Whittier, P.S., Choi, D., and Funk, W.D. (1999). Microarray analysis of replicative senescence. Curr. Biol. *9*, 939–945.

Storer, M., Mas, A., Robert-Moreno, A., Pecoraro, M., Ortells, M.C., Di Giacomo, V., Yosef, R., Pilpel, N., Krizhanovsky, V., Sharpe, J., and Keyes, W.M. (2013). Senescence is a developmental mechanism that contributes to embryonic growth and patterning. Cell. Published online November 14, 2013. http://dx.doi.org/10.1016/j.cell.2013.10.041.

Toledo, L.I., Murga, M., Gutierrez-Martinez, P., Soria, R., and Fernandez-Capetillo, O. (2008). ATR signaling can drive cells into senescence in the absence of DNA breaks. Genes Dev. *22*, 297–302.

Vazquez, M.D., Bouchet, P., Mallet, J.L., Foliguet, B., Gérard, H., and LeHeup, B. (1998). 3D reconstruction of the mouse's mesonephros. Anat. Histol. Embryol. *27*, 283–287.

Vousden, K.H., and Prives, C. (2009). Blinded by the light: the growing complexity of p53. Cell *137*, 413–431.

Xue, W., Zender, L., Miething, C., Dickins, R.A., Hernando, E., Krizhanovsky, V., Cordon-Cardo, C., and Lowe, S.W. (2007). Senescence and tumour clearance is triggered by p53 restoration in murine liver carcinomas. Nature *445*, 656–660.

Zoncu, R., Efeyan, A., and Sabatini, D.M. (2011). mTOR: from growth signal integration to cancer, diabetes and ageing. Nat. Rev. Mol. Cell Biol. *12*, 21–35.